

Pro-drug strategies to leverage transporters



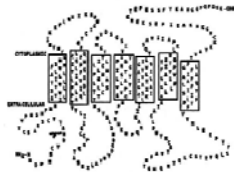
James E. Polli
October 6, 2011

Topics

- Apical Sodium-dependent Bile Acid Transporter (ASBT)
- Prodrugs
- Bile Acid Derivatives and SAR of Transporter
- Methods
- Solute Carrier Transporters in Drug Interactions
 - Drug inhibition of the bile acid transporter in the ileum to potentially cause colon cancer
 - Drug inhibition of OCTN2 transporter to potentially contribute to rhabdomyolysis

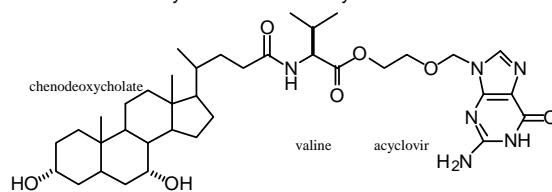
hASBT

- human Apical Sodium-dependent Bile Acid Transporter (SLC10A2)
- 7 TMD; 348 amino acids with a single glycosylation site at Asn¹⁰
- expressed in the ileum and involved in bile acid re-absorption
 - also expressed in kidney and cholangiocytes



hASBT Prodrug: Acyclovir Valylchenodeoxycholate

- Attributes
 - hASBT-mediated transport
 - Hydrolysis catalyzed by esterase to liberate acyclovir
 - Doubled acyclovir bioavailability in rat



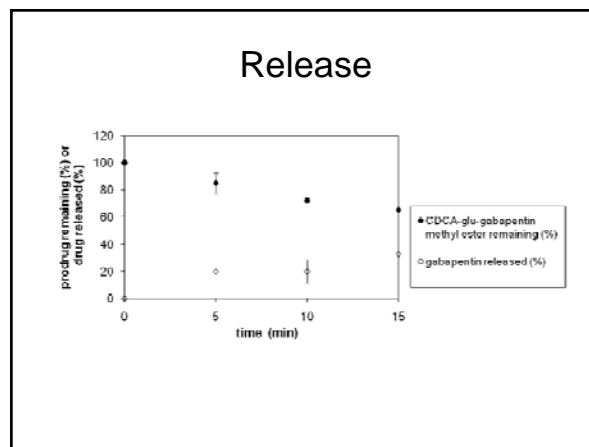
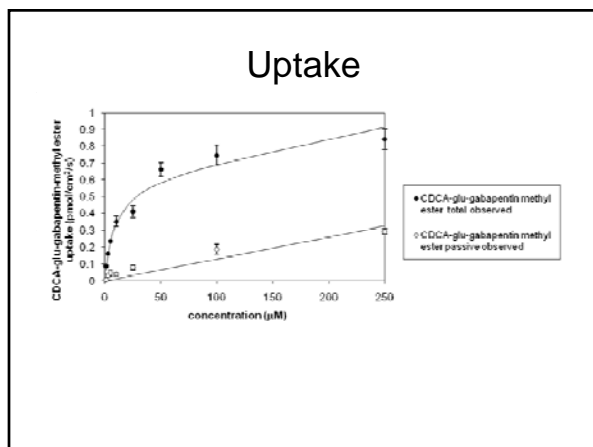
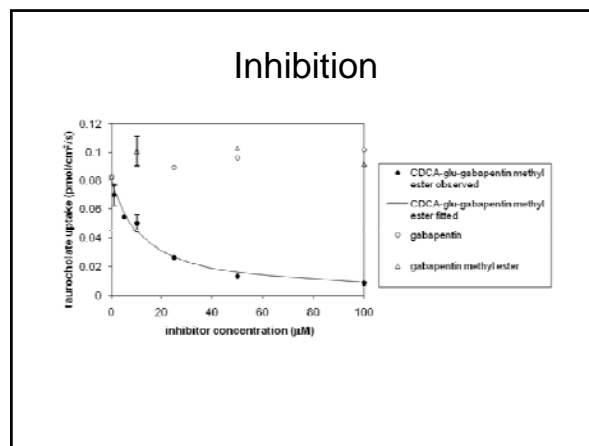
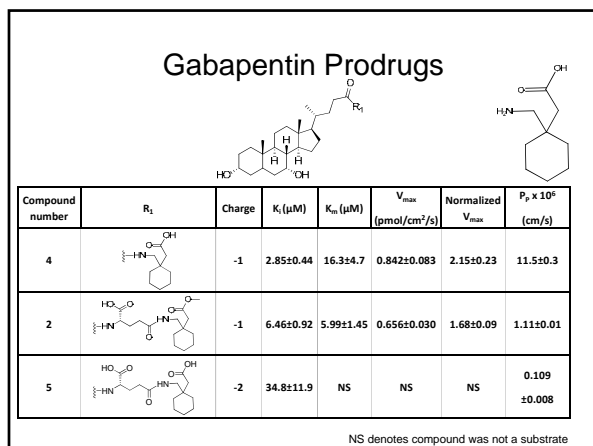
Tolle-Sander et al. (2004): Increased acyclovir oral bioavailability via a bile acid conjugate. *Mol. Pharmaceutics* 1:40-48.

Urinary Acyclovir Excretion after Oral Administration

Rat	Percent acyclovir recovered after acyclovir dose	Percent acyclovir recovered after acyclovir valylchenodeoxycholate dose	Recovery ratio of acyclovir from prodrug versus acyclovir
A	15.5	34.9	2.25
B	21.6	38.5	1.78
C	24.4	42.7	1.75
D	20.6	24.3	1.18
E	26.3	69.0	2.63
F	22.9	67.3	2.94
G	24.1	43.1	1.79
H	41.3	63.9	1.55
Mean	24.6 (±2.5)	48.0 (±5.6)	1.98 (±0.19)

Gabapentin Prodrugs

- Gabapentin is a structural analogue of gamma-amino butyric acid (GABA)
- Indicated to treat neuropathic pain and used as adjunctive therapy for partial seizures in adults with epilepsy
- Dose dependent pharmacokinetics
 - 60% at a 300 mg dose to about 35% or less at 1000 mg dose
- Low capacity (and saturable) amino acid transporters involved gabapentin uptake in upper small intestine



Extended Release

- **Niacin** - slower availability reduces flushing side effect

- **Ketoprofen** - GI side effect and short half-life of 2 hr

Zheng, X. and Poll, J.E. (2010): Synthesis and In Vitro Evaluation of Potential Sustained Release Prodrugs via Targeting ASBT. Int. J. Pharm., 396: 111–118.

Approach and Findings

Synthesis

- Bile acid conjugates were potent inhibitors of ASBT

Inhibition Study

- CDCA-lysine-niacin showed high ASBT substrate binding affinity, but lower capacity compared to taurocholate

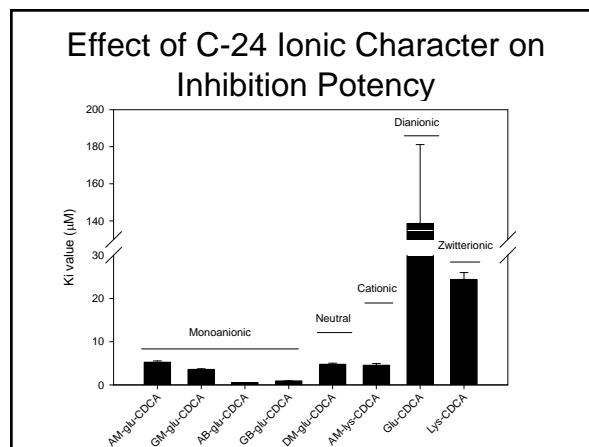
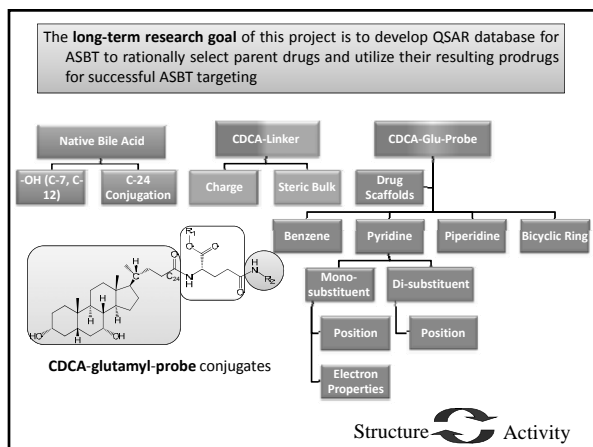
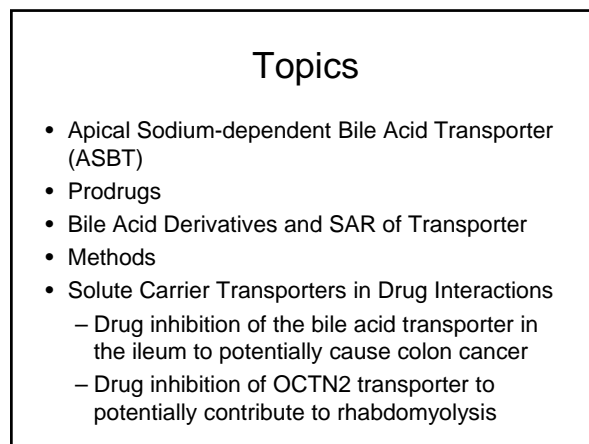
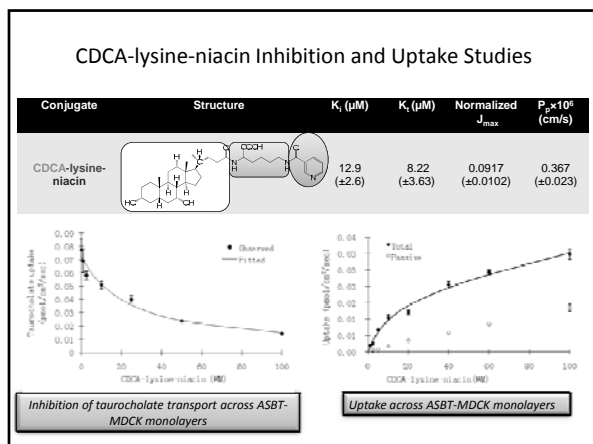
Uptake Study

- CDCA-lysine-ketoprofen was a weaker substrate

Stability Study

- Caco-2 cell homogenate
- Liver homogenate

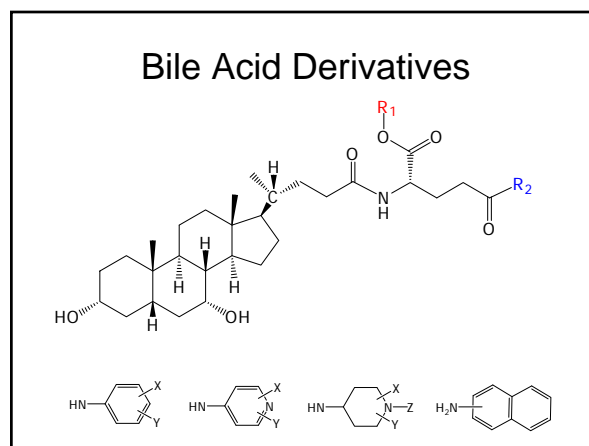
- Slow release of parent drug



C-24 chemistry effect on inhibitory potency and transport affinity

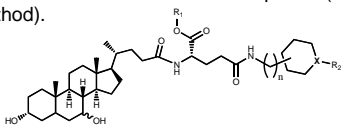
Ionic character	Conjugate	Inhibition potency	Substrate Affinity
Dianionic	Glu-CDCA	Low	Non-substrate
Monoanionic	AM-glu-CDCA	High	Substrate
	AB-glu-CDCA	High	Substrate
	GM-glu-CDCA	High	Substrate
	GB-glu-CDCA	High	Substrate
Cationic	AM-Lys-CDCA	High	Non-substrate
Zwitterionic	Lys-CDCA	Moderate	Non-substrate
Neutral	DM-glu-CDCA	High	nd

Inhibition potency: Low, moderate, and high are $K_i > 100\mu\text{M}$, $100\mu\text{M} > K_i > 10\mu\text{M}$, and $K_i < 10\mu\text{M}$. nd = not determinable owing to high passive permeability



Aminopiperidine conjugates

- Aminopiperidine conjugates of glutamyl-chenodeoxycholate (glu-CDCA) and glutamyl-ursodeoxycholate (glu-UDCA)
- 3-D QSAR model based on CSP method (CSP-SAR) to determine structural hASBT-binding requirements
 - All possible conformations sampled by a molecule were considered for model development (CSP method).

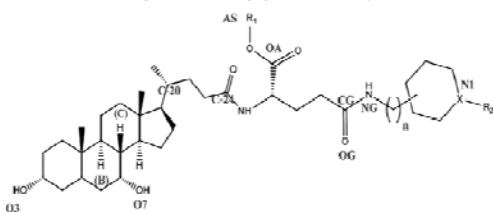


González, P.M., Acharya, C., MacKerell Jr., A.D., and Polli, J.E. (2009): Inhibition Requirements of the human Apical Sodium-dependent Bile acid Transporter (hASBT) using Aminopiperidine Conjugates of glutamyl-Bile Acids. *Pharm. Res.* 26:1665-1678.

Conformationally Sampled Pharmacophore Approach (CSP-SAR)

- All possible conformations sampled by each molecule were considered for model development (CSP method)
- e.g. K_i as a linear function of structural and physical properties
- Combinations of descriptors with internal correlation < 0.80 selected as candidate models
- AIC criteria to identify the best model among competing models (ranking of models)
- Leave-one-out cross-validation (Q^2) for model validation

Conformationally Sampled Pharmacophore Approach (CSP-SAR)



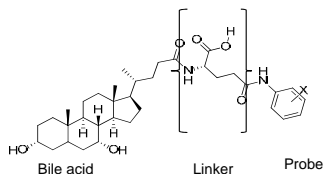
- Properties that favor hASBT inhibition:
 - Increased hydrophobicity
 - Close proximity of the piperidine moiety to the cholestane skeleton (distance N1-O7), but not a salt bridge
 - Partially compacted side chain (angle C20-N1-OA)

Results

- Potent inhibitors of hASBT (K_i 0.953 - 31.8 μ M)
- Esterification of the α -acid did not decrease inhibitory potency
 - negative charge not necessary
- CSP-SAR model suggests that bile acid conjugates with N1 lying within 6-7 Å from OA is preferred for binding.

Aniliny conjugates of glu-CDCA

- Substituent variables:
 - Location, electronic character, size

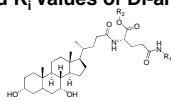


Rais, R., Acharya, C., MacKerell Jr., A.D., and Polli, J.E. (2010): Molecular switch controlling the binding of anionic bile acid conjugates by hASBT. *J. Med. Chem.* 53: 4749-4760

Inhibition Results

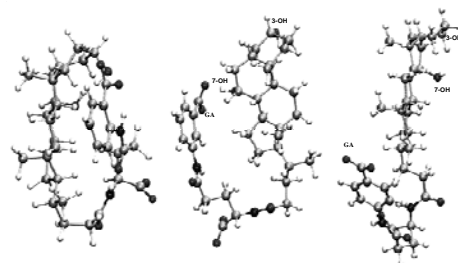
- Thirty-three aniliny conjugates of glu-CDCA provided K_i from 0.275 to 108 μ M
 - All monoanionic conjugates were potent inhibitors (K_i between 0.275 to 15.9 μ M)
- Presence of charge (on gamma substituent) distal to C-24 did not affect the binding affinity
- Amongst the dianionic conjugates, 2ABA and 3ABA were found to be more potent than 4ABA
- Three quantitative CSP-SAR models that excluded the weak dianion 4ABA were developed and identified physico-chemical features that favor binding
- A qualitative CSP-SAR model was derived to explain affinity values of the dianionic molecules, including 4ABA
- A "molecular switch" associated with the spatial location of the carboxylate group on the aromatic ring, controlled intramolecular hydrogen bonding and hence activity

Structures and K_i Values of Di-anionic Conjugates of Glu-CDCA



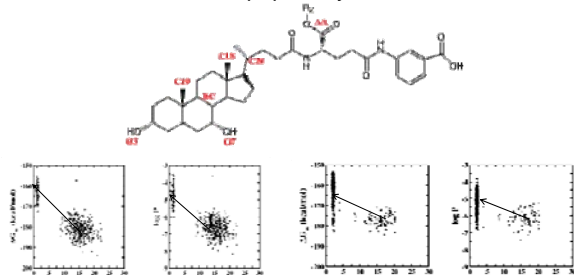
Compound	R ₁	R ₂	Charge	Observed K_i (pM)	Predicted K_i (pM) ^a
2ABA (31)		H	-2	40.4±5.7	40.1
3ABA (32)		H	-2	35.9±3.5	35.3
4ABA (33)		H	-2	108±8	No fit model
3ABAM (34)		H	-2	126±13	No fit model
4ABAM (35)		H	25	41.0±4.1	39.6

Qualitative Model for Dianions



Representative conformers of 2ABA, 3ABA and 4ABA, illustrating the intramolecular hydrogen bond in 2 and 3ABA, but not in 4ABA.

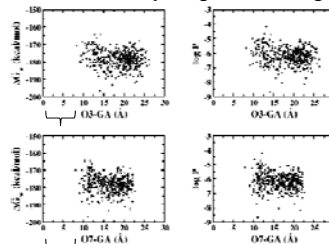
2ABA and 3ABA: Lipophilicity and Conformation



The change in ΔG_w and $\log P$ as a function of the distance between 3-OH and γ -acid (O3-GA) for **2ABA**

The change in ΔG_w and $\log P$ as a function of the distance between 7-OH and γ -acid (O7-GA) for **3ABA**

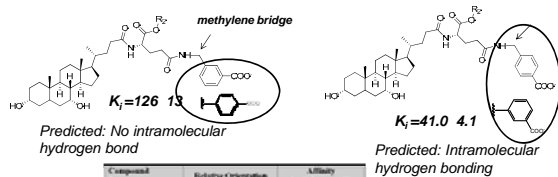
4ABA: No hydrogen bonding



The change in ΔG_w and $\log P$ as a function of O3-GA (distance between 3-OH and γ -acid) and O7-GA (distance between 7-OH and γ -acid) for **4ABA**

No hydrogen bonding or associated change in physicochemical properties

Model Validation: Molecular Switch Hypothesis

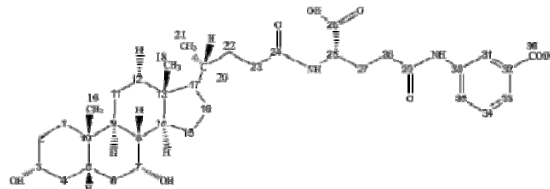


Predicted: No intramolecular hydrogen bond

Predicted: Intramolecular hydrogen bonding

Compound number	Behavioral Characteristic	Affinity (pM) (30, 35, 40, 45)
32		High (30)
33		Intermediate (35)
34		Low (40)
35		High (45)

Model Validation: Differences Between 3ABA and 4ABA by 1D Saturated NOE NMR



Model Validation: Differences Between 3ABA and 4ABA by 1D Saturated NOE NMR

Compound Number	Proton Irradiated*	Observed NOE Enhancement from NMR studies*	Shortest Distance from MD Simulations (Å)
3ABA	31	18	3.61
		19	5.45
		21	4.90
	35	18	3.34
		19	3.28
		21	4.99
	21	31	4.90
		18	1.82
	18	19	5.16
		31	3.61
21		1.82	
19		2.11	
33	34	2.10	
	18 (weak)	4.54	
4ABA	21 (weak)	5.97	
	31	32	2.13
	32	31	2.13
	18	None	∅
	19	None	∅
21	None	∅	

NOE's observed between aromatic protons and steroid ring for 3ABA. No NOE's for 4ABA.

Topics

- Apical Sodium-dependent Bile Acid Transporter (ASBT)
- Prodrugs
- Bile Acid Derivatives and SAR of Transporter
- Methods
- Solute Carrier Transporters in Drug Interactions
 - Drug inhibition of the bile acid transporter in the ileum to potentially cause colon cancer
 - Drug inhibition of OCTN2 transporter to potentially contribute to rhabdomyolysis

Methods

- Bias in K_t and J_{max} estimates from transport studies: interplay of transporter expression level and substrate affinity
 - and in K_i from inhibition studies
- Impact of impurity on kinetic estimates from transport and inhibition studies
- Co-solvents and methods to screen for transporter substrate
- Identification of inhibitor concentrations to efficiently screen and measure K_i
- Reliability of inhibition models to correctly identify type of inhibition

Topics

- Apical Sodium-dependent Bile Acid Transporter (ASBT)
- Prodrugs
- Bile Acid Derivatives and SAR of Transporter
- Methods
- Solute Carrier Transporters in Drug Interactions
 - Drug inhibition of the bile acid transporter in the ileum to potentially cause colon cancer
 - Drug inhibition of OCTN2 transporter to potentially contribute to rhabdomyolysis

Bile Acids Cause Colon Cancer

- In rodents, feeding secondary bile acids increases colon epithelial dysplasia risk.
- In rodents, feeding ursodeoxycholate reduces fecal deoxycholate and reduces colon tumor formation.
- In humans with IBD, feeding ursodeoxycholate reduces fecal deoxycholate and reduces colon epithelial dysplasia and cancer.

Purpose:

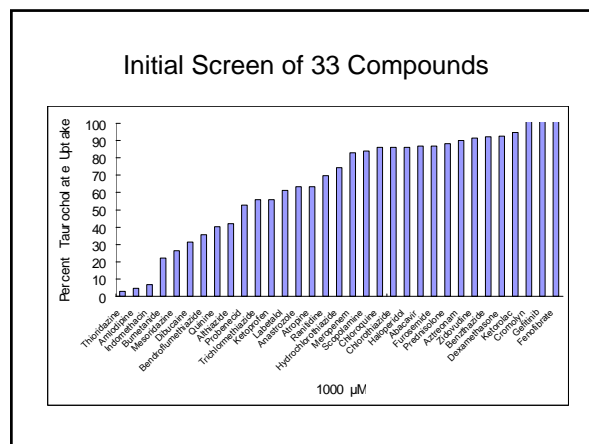
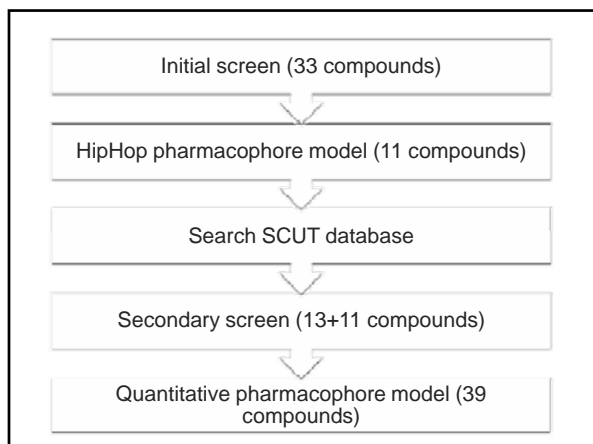
- The purpose of this study was to identify drugs that inhibit hASBT and develop a pharmacophore model of hASBT.

Inhibition Studies:

- Compounds were evaluated for binding to hASBT via inhibition of 2.5 μM taurocholate (TCA) with 1 μCi ³H-TCA uptake into hASBT-MDCK monolayers.

Inhibition Constant K_i Determination:

- Eight concentrations of each compound
- K_i were estimated by non-linear regression



Inhibition Results from Initial Screen

Compound	Taurocholate Uptake in Presence of 1000 µM Compound	K _i Value (µM)
Thioridazine	2.9	37.3±4.0
Amlodipine	4.5	42.1±7.7
Indomethacin	6.8	62.3±4.6
Bumetanide	21.9	225±17
Mesoridazine	26.4	17.6±2.3
Dibucaine	31.2	34.7±4.9
Bendroflumethiazide	35.5	92.7±12.7
Quinine	40.1	223±25
Aithiazide	42.1	377±79
Probenecid	52.6	385±81
Trichlormethiazide	55.7	377±79

- Initially 33 compounds screened.
- 11 compounds showed the greatest inhibition of taurocholate.
- These 11 compounds were used as a training set to generate a HipHop pharmacophore.

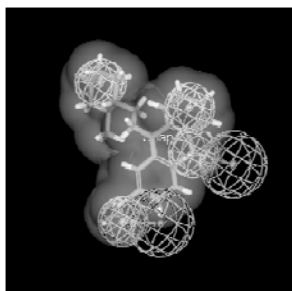
Inhibition Results from Initial Screen (continued)

Inhibition result 2 from Initial Screen Study

Compounds	Taurocholate uptake in presence of 1000 µM compound	K _i Value (µM)
Ketoprofen	56.0	178±29
Labeltalol	61.4	851±104
Anastrozole	63.2	402±43
Atropine	63.5	170±22
Ranitidine	69.8	886±158
Hydrochlorothiazide	74.2	1220±140
Chlorothiazide	83.2	2020±330
Scopolamine	84.1	6450±1120
Chloroquine	86.0	6320±150
Abacavir	86.9	5020±880
Meropenem	89.8	5010±2600

- Additionally, 11 compounds weakly inhibited taurocholate.
- 11 compounds did not show inhibition activity.

HipHop Pharmacophore Model



- A common feature HipHop pharmacophore model of hASBT was generated from the 11 most potent inhibitors.
- The most active compound **mesoridazine** was used to create a shape restriction.
- The model consisted of:
 - 2 hydrogen bond acceptors (Green)
 - 2 hydrophobes (Blue)

Inhibition Result from Secondary Screen

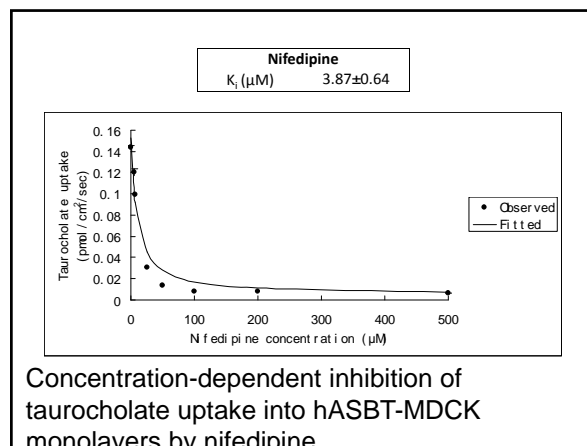
Compound	Fit Value	K _i Value (µM)
Thiothixene	3.758	808±98
Indomethacin*	3.254	62.3±4.6
Doxorubicin	3.142	101±21
Enalapril	3.049	NA
Aztreonam**	2.973	NA
Bumetanide*	2.929	225±17
Mesoridazine*	2.871	17.6±2.3
Nimodipine	2.829	5.75±0.72
Amlodipine*	2.82	42.1±7.7
Lansoprazole	2.566	60.0±7.6
Fluvastatin	2.565	11.5±0.8
Thioridazine*	2.314	37.3±4.0
Toraseamide	2.277	414±86
Latanoprost	2.047	11.0±2.0
Lovastatin	1.733	21.6±2.3
Pentamidine	1.541	76.3±19.2
Simvastatin	1.503	10.4±2.1
Furosemide**	0.959	NA
Pioglitazone	0.688	NA
Tioconazole	0.5	33.1±2.7

- The HipHop pharmacophore was used to search the SCUT database. 58 hits were retrieved:
 - 5 from the training set (*)
 - 2 were not inhibitors from initial screen (**)
- 13 new compounds were selected for *in vitro* inhibition:
 - 11 inhibited
 - K_i: 5.75 µM - 808 µM
 - two did not inhibit: enalapril and pioglitazone

Inhibition Result of Calcium Channel Blockers and HMG CoA-reductase Inhibitors

Compound	Drug Class	K_i Value (μM)
Nifedipine	Dihydropyridine-calcium channel blocker	3.87±0.64
Nisoldipine	Dihydropyridine-calcium channel blocker	4.77±1.05
Nimodipine*	Dihydropyridine-calcium channel blocker	5.75±0.72
Simvastatin*	Statin-HMG CoA-reductase inhibitors	10.4± 2.1
Fluvastatin*	Statin- HMG CoA-reductase inhibitors	11.5±0.8
Isradipine	Dihydropyridine-calcium channel blocker	19.4±3.0
Lovastatin*	Statin-HMG CoA-reductase inhibitors	21.6±2.3
Nemadipine	Dihydropyridine-calcium channel blocker	23.1±4.1
Nicardipine	Dihydropyridine-calcium channel blocker	32.4±3.1
Nitrendipine	Dihydropyridine-calcium channel blocker	34.1± 5.1
Amlodipine*	Dihydropyridine-calcium channel blocker	42.1±7.7
Felodipine	Dihydropyridine-calcium channel blocker	49.7±7.0
Diltiazem	Benzothiazepines-calcium channel blocker	211±21
Verapamil	Phenylalkylamine-calcium channel blocker	266±22

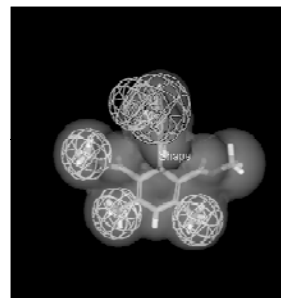
- Most potent inhibitors were calcium channel blockers (nimodipine) and HMG CoA-reductase inhibitors (fluvastatin)
- Ten additional calcium channel blockers were studied.
- Dihydropyridines are more potent hASBT inhibitors than other classes of calcium channel blockers .



Training Set (39 compounds) for Quantitative Pharmacophore Model

Compound	K_i Value (μM)	Compound	K_i Value (μM)
Nifedipine	3.87±0.64	Bendroflumethiazide	92.7±12.7
Nimodipine	5.75±0.72	Doxorubicin	101±21
Simvastatin	10.4± 2.1	Spirooctone	110±17
Latanoprost	11.0±2.0	Atropine	170 ±22
Fluvastatin	11.5±0.8	Ketoprofen	178±29
Mesoridazine	17.6±2.3	Diltiazem	211±21
Isradipine	19.4±3.0	Quinine	223±25
Lovastatin	21.6±2.3	Bumetanide	225±17
Nemadipine	23.1±4.1	Triclometiazide	377±79
Nicardipine	32.4±3.1	Probenecid	385 ±81
Tioconazole	33.1±2.7	Althiazide	391±56
Nitrendipine	34.1± 5.1	Anastrozole	402±43
Dibucaine	34.7±5.0	Thiothixene	808 ±98
Thioridazine	37.3±4.0	Labetalol	851 ±104
Amlodipine	42.1±7.7	Ranitidine	886 ±158
Felodipine	49.7±7.0	Meropenem	5000±2560
Lansoprazole	60.0±7.6	Abacavir	5020±880
Propafenone	62.0± 6.7	Chloroquine	6320±150
Indomethacin	62.3±4.6	Scopolamine	6450±1120
Pentamidine	76.3±19.2		

Quantitative Pharmacophore Model



- A quantitative pharmacophore was generated with 39 compounds using the HypoGen method
- **Nifedipine** was used to map to the pharmacophore to create a shape restriction.
- The model consisted of:
 - 1 hydrogen bond acceptors (Green)
 - 3 hydrophobes (Blue)
- $r^2 = 0.664$

hASBT Conclusions

- A large number of drugs from diverse classes were found to be hASBT inhibitors.
- Most potent inhibitors were dihydropyridine calcium channel blockers, HMG CoA-reductase inhibitors, or diuretics.
- Future pharmacoeconomic studies will attempt to elucidate a possible relationship between hASBT inhibition and the incidence of colon cancer.
- Zheng, X., Ekins, S., Raufman, J., and Polli, J.E. (2009): Computational models for drug inhibition of the human apical sodium-dependent bile acid transporter. *Mol. Pharmaceutics* 5:1591-1603.

Topics

- Apical Sodium-dependent Bile Acid Transporter (ASBT)
- Prodrugs
- Bile Acid Derivatives and SAR of Transporter
- Methods
- Solute Carrier Transporters in Drug Interactions
 - Drug inhibition of the bile acid transporter in the ileum to potentially cause colon cancer
 - Drug inhibition of OCTN2 transporter to potentially contribute to rhabdomyolysis

OCTN2:
Organic Cation/carnitine Transporter

Solute carrier family 22 (organic cation transporter), member 5

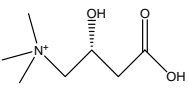
L-carnitine

Widespread expression: kidney, heart, muscle, placenta, small intestine

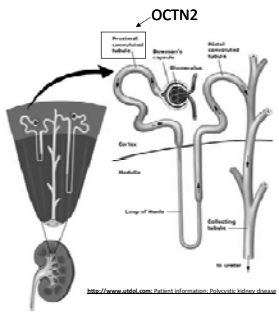
High affinity Na⁺-dependent transporter for L-carnitine, which is required for the transport of fatty acids into mitochondria to generate energy.

OCTN2 mutations in humans cause a low L-carnitine level in plasma and tissues and induce significant clinical symptoms such as progressive cardiomyopathy, skeletal myopathy, hypoketotic hypoglycaemic encephalopathy: Primary Carnitine Deficiency

Significant physiological and pharmacological implications



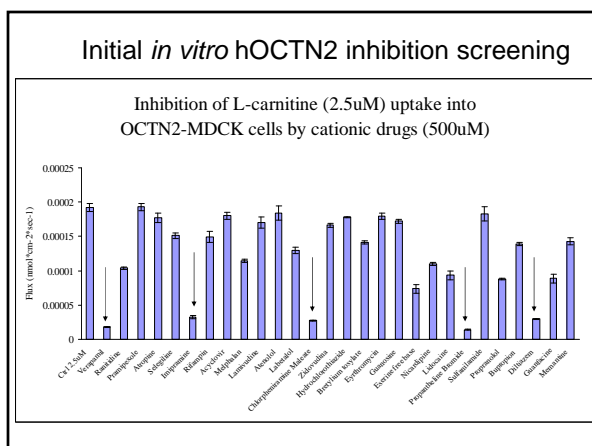
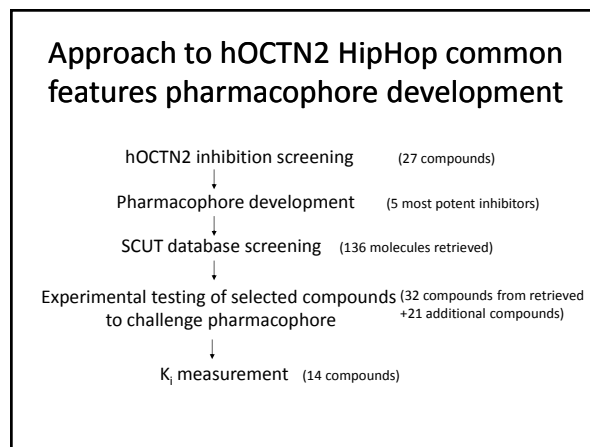
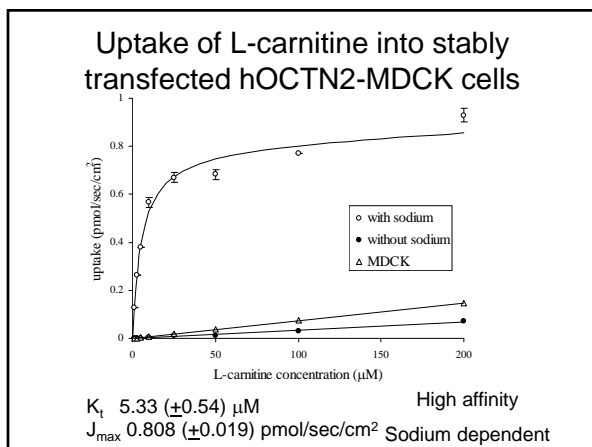
OCTN2 Re-absorbs L-carnitine



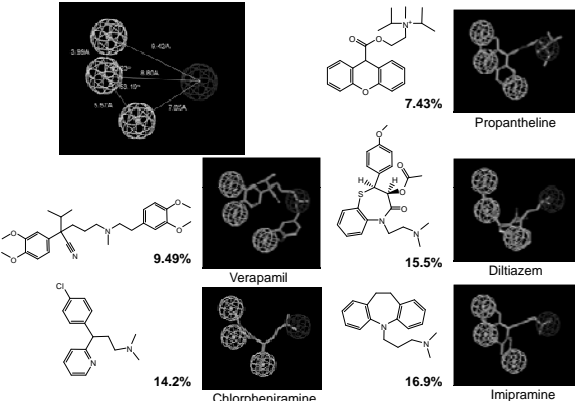
The inhibition of carnitine renal re-absorption implicated as the possible mechanism for drug induced carnitine deficiency.

Possible association between clinical rhabdomyolysis and OCTN2 inhibition.

Inhibition requirements of hOCTN2 to potentially predict drug-induced toxicity and carnitine deficiency.



HipHop common features pharmacophore model for hOCTN2 inhibition



- Propranolol: 7.43%
- Verapamil: 9.49%
- Chlorpheniramine: 14.2%
- Diltiazem: 15.5%
- Imipramine: 16.9%

32 drugs tested *in vitro*, selected from 136 drugs retrieved by the pharmacophore from SCUT database

Compound name	FitValue	Percent L-carnitine uptake compared to control	Compound name	FitValue	Percent L-carnitine uptake compared to control
Thioridazine	3.598	0.375±0.017	Chloroquine	2.839	44.6±1.0
Vinblastine	3.58	3.38±0.22	Metoclopramide	2.692	11.5±0.8
Clozapine	3.54	9.38±0.27	Desloratadine	2.674	6.97±0.219
Amlodipine	3.527	14.4±0.5	Duloxetine	2.595	15.6±0.7
Gefitinib	3.479	7.90±0.18	Carvedilol	2.593	5.64±0.34
Trifluoperazine	3.408	0.24±0.01	Vancomycin	2.577	54.4±1.7
Dibucaine	3.404	26.3±1.3	Olanzapine	2.432	32.0±0.9
Tamoxifen	3.348	5.67±0.05	Amitriptyline	2.149	22.5±0.7
Amlodarone	3.331	1.70±0.09	Gemifloxacin	1.796	67.8±0.4
Atracurium	3.292	36.8±2.7	Imatinib	1.759	3.98±0.22
Nefazodone	3.243	4.53±0.14	Desipramine	1.612	32.4±0.8
Argatroban	3.223	39.1±1.9	Sildenafil	1.587	69.7±2.8
Pentamidine	3.083	77.2±1.9	Quinine	1.343	14.3±0.5
Nelfinavir	3.005	8.07±0.10	Quinidine	0.955	17.2±0.6
Prochlorperazine	3.002	0.318±0.032	Haloperidol	0.788	26.0±1.2
Raloxifene	2.954	1.65±0.13	Bromocriptine	0.448	2.59±0.09

Diverse therapeutic classes of drugs found as novel low micromolar inhibitors of OCTN2. 27 drugs (84.4%) found to be potent inhibitors (i.e. 40% or less L-carnitine uptake). Pharmacophore prediction has a low false positive rate (15.6%).

Compound name	FitValue	Percent L-carnitine uptake compared to control
Emetine	3.857	46.9±2.8
Mirtazapine	No map	27.8±2.3
Betaine	No map	40.5±0.2
Cerivastatin	No map	43.4±2.1
Pyrilamine	No map	51.7±1.6
Citalopram	No map	52.6±2.0
Cephalexin	No map	53.2±0.8
Cimetidine	No map	54.1±2.6
Atorvastatin	No map	57.2±2.0
Edrophonium	No map	60.1±1.0
Venlafaxine	No map	69.9±3.1
Bethanechol	No map	74.1±1.6
Choline	No map	76.0±2.2
Cyclopentolate	No map	76.9±2.2
Ketorolac	No map	82.1±0.4
Gabapentin	No map	83.0±3.5
Levofloxacin	No map	85.0±0.3
Succinylcholine	No map	89.0±2.1
Lomefloxacin	No map	92.3±5.2
Procabazine	No map	88.3±2.8
Lisinopril	No map	114±3

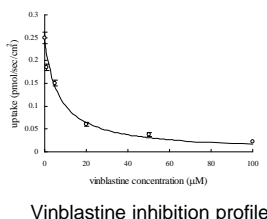
Additional tested 21 compounds: Carnitine mimics; Compounds previously reported to inhibit OCTN2; Drugs that cause rhabdomyolysis

Among the 20 compounds not mapping to the pharmacophore, only one (5%) is potent inhibitor.

Pharmacophore prediction has a low false negative rate (5%).

14 compounds competitive K_i determined

Compound name	FitValue	Competitive inhibitory K_i value (μ M)
Vinblastine	3.580	4.85±0.71
Carvedilol	2.593	10.7±1.6
Raloxifene	2.954	13.8±2.4
Bromocriptine	0.448	16.6±2.0
Verapamil	3.714	17.6±3.1
Propranolol	1.4	20.4±4.1
Thioridazine	3.598	23.0±4.1
Clozapine	3.540	47.3±8.6
Prochlorperazine	3.002	51.3±10.5
Desloratadine	2.674	53.3±6.7
Trifluoperazine	3.408	67.3±10.1
Amlodipine	3.527	96.0±15.2
Duloxetine	2.595	118±13
Cerivastatin	No map	425±12



Possible association between clinical rhabdomyolysis and hOCTN2 inhibition

Compound name	K_i or estimated K_i (μ M)	Documented to cause Rhabdomyolysis in the literature	C_{max} (μ M)	C_{max}/K_i	Compound name	K_i or estimated K_i (μ M)	Documented to cause Rhabdomyolysis in the literature	C_{max} (μ M)	C_{max}/K_i
Amiodarone	5.72	Yes with Simvastatin	3.43	0.600	Ketorolac	1530	No	3.36	0.00220
Nelfinavir	28.2	Yes with Simvastatin	10.2	0.349	Acyclovir	5130	No	7.16	0.00140
Thioridazine	23.0±4.1	Yes	6.75	0.293	Vinblastine	4.85±0.71	No	0.00064	0.00125
Nefazodone	15.7	Yes with Simvastatin	2.62	0.167	Pricalcainine	2530	No	3.13	0.00124
Risperidone	11.68	No	8.32	0.0717	Suboxone	118±13	No	0.122	0.00103
Succinylcholine	2700	Yes	130	0.0487	Erythromycin	2870	Yes with Simvastatin	2.23	7.77×10 ⁻⁷
Propranolol	20.4±4.1	No	1.06	0.0519	Desloratadine	53.3±6.7	No	0.0335	6.28×10 ⁻⁴
Cerivastatin	425±12	Yes	19.6	0.0461	Hydrochlorothiazide	4110	No	1.65	4.01×10 ⁻⁴
Clozapine	47.3±8.6	Yes	1.72	0.0364	Prochlorperazine	51.3±10.5	No	0.0168	3.27×10 ⁻⁴
Verapamil	17.6±3.1	Yes with Transdolipri	0.306	0.0174	Atenolol	8000	No	1.13	1.41×10 ⁻⁴
Gefitinib	29	No	0.474	0.0164	Raloxifene	13.8±2.4	No	0.00148	1.07×10 ⁻⁴
Carvedilol	10.7±1.6	No	0.131	0.0123	Amlodipine	96.0±15.2	No	0.000810	8.41×10 ⁻⁵
Tamoxifen	20	No	0.171	0.00854	Trifluoperazine	67.3±10.1	No	0.00528	7.85×10 ⁻⁵
Levofloxacin	1900	Yes	14.4	0.00756	Bromocriptine	16.6±2.0	No	0.000959	5.78×10 ⁻⁵
Lomefloxacin	4000	No	10.5	0.00283	Sildenafil	1230	Yes	0.0244	1.98×10 ⁻⁵
Lamivudine	2590	Yes	6.67	0.00258	Atropine	4000	No	0.0132	8.30×10 ⁻⁶
				C_{max}/K_i 0.0025	Zidovudine	2140	No	0.0124	5.76×10 ⁻⁶

Possible association between clinical rhabdomyolysis and hOCTN2 inhibition

- Among the 12 compounds associated with rhabdomyolysis, 10 (83.3%) have a C_{max}/K_i ratio higher than 0.0025.
- Among 21 compounds not associated with rhabdomyolysis, only six (28.6%) have a C_{max}/K_i ratio higher than 0.0025.
- Clinical rhabdomyolysis was associated with a C_{max}/K_i value above 0.0025 (Pearson's chi-square test $p=0.00247$).

hOCTN2 Conclusions

- Qualitative common features HIPHOP model developed for hOCTN2 inhibition
- Diverse therapeutic classes of drugs found to be novel potent hOCTN2 inhibitors
- Possible association of rhabdomyolysis and hOCTN2 inhibition

Topics

- Apical Sodium-dependent Bile Acid Transporter (ASBT)
- Prodrugs
- Bile Acid Derivatives and SAR of Transporter
- Methods
- Solute Carrier Transporters in Drug Interactions
 - Drug inhibition of the bile acid transporter in the ileum to potentially cause colon cancer
 - Drug inhibition of OCTN2 transporter to potentially contribute to rhabdomyolysis

Acknowledgements

- Sanna Tolle
- Anand Balakrishnan
- Pablo Gonzalez
- Gasirat Tririya
- Chayan Acharya
- Rana Rais
- Xiaowan Zheng
- Alex MacKerell
- Peter Swaan
- Sean Ekins
- Andy Coop
- NIH DK067530